

Scaling Behavior of the rf Vortex Penetration Depth in an Organic Superconductor

S. Sridhar, B. Maheswaran, Balam A. Willemsen, and Dong Ho Wu
Department of Physics, Northeastern University, Boston, Massachusetts 02115

R. C. Haddon

AT&T Bell Laboratories, Murray Hill, New Jersey 07974

(Received 31 December 1991)

The radio-frequency penetration depth $\lambda(H, T)$ of the organic superconductor $(\text{BEDT-TTF})_2\text{Cu}(\text{NCS})_2$ was studied in the mixed state at moderate fields. Data can be scaled into a single functional form $\Delta\lambda(H, T) = \Delta\lambda^*(T)f(H/H^*(T))$, where $H^*(T) \propto (1-t)^{3/2}/t$ can be identified with a "depinning" or "irreversibility" line. We show that the scaling features are contained in a theory of vortex motion in a periodic potential under the influence of thermal fluctuations, which describes the functional form quantitatively. Data for $\Delta\lambda(H=0, T)$ are governed by the same (vortex) length scale as finite-field data, suggesting that the zero-field state is not a conventional Meissner state obeying a London relation.

PACS numbers: 74.60.Ge, 74.30.Ci, 74.60.Ec, 74.70.Kn

Recently, significant developments [1] have occurred among organic superconductors with T_c 's attaining "record" highs exceeding 11 K. Equally important and of fundamental scientific interest are the unusual properties of these organic superconductors. It has been suggested that one organic superconductor, $(\text{BEDT-TTF})_2\text{Cu}(\text{NCS})_2$, has a p -wave superconducting state [2], although other measurements [3,4] indicate conventional s -wave superconductivity. The strongly two dimensional nature of the material has been demonstrated by torque measurements [5]. Even the normal state has been shown [6] to have unusual properties, related to the two dimensionality. From a theoretical viewpoint [7], these materials appear to be "a complete mystery."

In this paper we present detailed results for the electromagnetic properties of one member of the BEDT family, viz. $(\text{BEDT-TTF})_2\text{Cu}(\text{NCS})_2$, at moderate fields in the mixed state. We find that the magnetic (H) and temperature (T) dependence of the vortex contribution to the radio frequency (6 MHz) penetration depth λ obey a remarkable scaling, in that the data can be represented as

$$\Delta\lambda(H, T) \equiv \lambda(T, H) - \lambda(T, 0) = \Delta\lambda^*(T)f(H/H^*(T)),$$

where $H^*(T) \propto (1-t)^{3/2}/t$. We analyze the results in terms of a theory [8] which studies the high-frequency dynamics of Abrikosov vortices in a periodic potential, under the influence of the ac driving force, and thermal fluctuations. We show that the observed scaling behavior is contained in this theory, which yields for the vortex contribution to the penetration depth a result $\lambda_r(H, \omega, T) = \delta^*(T)h(\omega\tau_0, H/H^*(T))$. The observed temperature dependence of the scaling field $H^*(T)$ is related to the H and T dependence of the pinning potential. Detailed numerical calculations for the scaling function are in good agreement with the experiments. In particular, a crossover from flux pinning to flux flow is observed which manifests itself as a characteristic knee in the field-dependent data, and which is accounted for by the theory. Thus $(\text{BEDT-TTF})_2\text{Cu}(\text{NCS})_2$ appears to be a typical type-II superconductor, with features of the vortex

response observed which should be characteristic of layered (e.g., cuprate) superconductors. These features are particularly pronounced in the BEDT superconductor because of the large length (e.g., λ) and low-field scales (e.g., H^*). Of equal interest is our finding that the $\lambda(H=0, T)$ data are governed by the same (vortex) length scale as the H -dependent data, which suggests that the zero-field state is not a conventional Meissner state (see discussion below).

Single-crystal samples fabricated at AT&T Bell Laboratories were grown following the procedure in Ref. [9]. The rf measurements were carried out using a tunnel-diode oscillator technique which has been extensively validated by measurements on both low- and high- T_c superconductors. In this technique, the frequency shift of the oscillator, which contains the sample in the inductance of the tank circuit, yields the penetration depth $\Delta\lambda(H, T) = -\zeta\Delta f(H, T)$. In experiments on $\text{YBa}_2\text{Cu}_3\text{O}_7$ (YBCO), the technique has been shown [10,11] to yield sensitive results on the penetration depth $\lambda(T, H)$, $H_{c1}(T)$, pair-breaking effects via the field derivative ($d\lambda/dH^2$), and flux-pinning forces κ_p .

Figure 1 presents $\Delta\lambda(T, H) \equiv \lambda(T, H) - \lambda(T, 0)$ for moderate applied fields at several temperatures below T_c (~ 9.9 K) for a single crystal of dimensions $1.2 \times 0.3 \times 0.03$ mm³. The rf probe field is applied parallel to the planes (b - c axes) and the dc field H is applied perpendicular to the planes (parallel to the \hat{a} axis). All the data shown in Fig. 1 are for a complete field cycle at each temperature; i.e., the field was increased up to about 3 kOe, then decreased through zero, and then increased in the opposite direction and subsequently reduced to zero. The curves are clearly symmetric about $H=0$. Although the data at first glance suggest a spectacular reversibility, a very slight hysteresis ($< 1\%$) does exist with reversal of field (i.e., field increasing versus decreasing), which is visible upon substantial vertical magnification.

The overall behavior of $\Delta\lambda(H)$ for the various temperatures is essentially identical, except for temperature-dependent vertical and horizontal (field) scales. A strik-

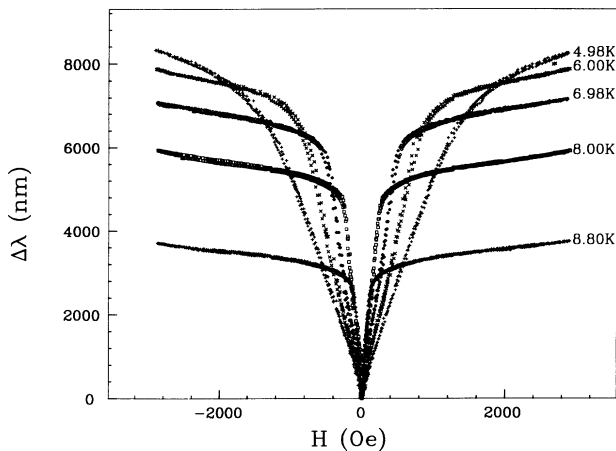


FIG. 1. $\Delta\lambda(H, T)$ vs H for various T .

ing feature is the enormous magnitude of the effects. Even for the relatively modest fields of Fig. 1, λ changes very strongly with field, and approaches large values very quickly. This behavior appears, at first glance, to be quite unlike that encountered in YBCO or the conventional superconductors at comparable (moderate) fields. However, as the subsequent discussion shows, the entire field dependence can be understood and is strongly influenced by the low-field scales and the large length scales relevant to the organic superconductor.

A remarkable feature of the data in Fig. 1 is that the T and H dependences can be completely described by a one-parameter scaling approach. In Fig. 2, we plot $\Delta\lambda(H, T)/\Delta\lambda^*(T)$ vs $H/H^*(T)$, where $H^*(T)$ is a temperature-dependent scaling field—the various curves in Fig. 1 are seen to collapse onto a single curve. As is apparent from Fig. 2, a one-parameter scaling represents the data over the entire temperature range.

The temperature dependence of the scaling field $H^*(T)$ is shown in Fig. 3. Clearly $H^*(T)$ has an upward curvature, and the temperature dependence is well represented by $H^*(T) = (1.9 \text{ kOe})(1 - t)^{3/2}/t$. This is strongly suggestive of the “irreversibility line,” first observed in YBCO by Müller, Takashige, and Bednorz [12], which has also been associated with a “depinning” field in penetration depth measurements in YBCO [13]. The scaling description and the field $H^*(T)$ are also reminiscent of the behavior [14,15] of the dc resistivity and magnetization in YBCO. We next show that the scaling behavior and the temperature dependence of the scaling field represented in Figs. 2 and 3 are contained in a theory which studies the high-frequency vortex response in the presence of thermal fluctuations.

In our configuration, the dc field $\mathbf{H} \parallel \hat{\mathbf{a}}$ (perpendicular to the planes) and the rf field H_ω and induced current J_ω are parallel to the planes. Thus the vortices are created perpendicular to the planes, and are driven parallel to the planes by the rf field or induced current. The experiment probes the reactive response of the vortices to the Lorentz

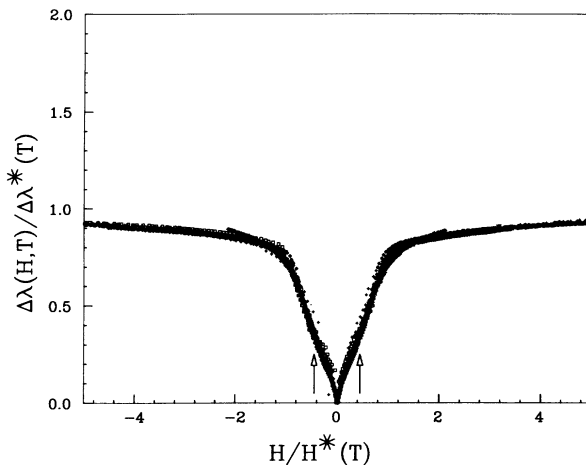


FIG. 2. Scaled presentation of the data in Fig. 1, i.e., $\Delta\lambda(H, T)/\Delta\lambda^*(T)$ vs $H/H^*(T)$. The arrows indicate the cross-over region.

force caused by the induced rf current. The equation of motion of individual vortices can be represented by

$$\eta \dot{x} + \kappa_p (L/2\pi) \sin(2\pi x/L) = \phi_0 J_\omega + \tilde{F}(t),$$

where η is the flux-flow viscosity and κ_p is the pinning force constant. \tilde{F} represents the Langevin force due to thermal activation of the vortices out of their pinning wells.

First we note that if we linearize the above equation, and ignore the effects of flux creep (i.e., the \tilde{F} term), one obtains a simple constitutive relation $J_\omega = [(\kappa_p + i\omega\eta)/i\omega\phi_0 B] E_\omega$, yielding for the penetration depth in the limit $\omega \rightarrow 0$

$$\lambda(H) = [\phi_0/\mu_0\kappa_p(T)]^{1/2} \sqrt{B(H)}. \tag{1}$$

In identical experiments on YBCO at low fields we have verified the predicted \sqrt{H} behavior of $\lambda(H)$ and from the slope extracted the pinning forces $\kappa_p(T)$ between 4.2 K

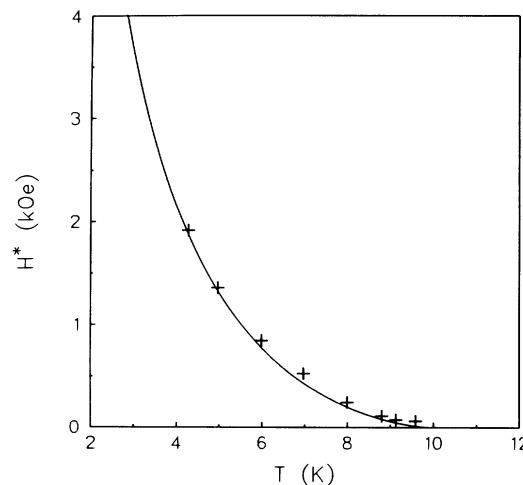


FIG. 3. $H^*(T)$ vs T . The solid line is a fit by $(1.9 \text{ kOe})(1 - t)^{3/2}/t$ with $T_c = 9.9 \text{ K}$.

and T_c in both \parallel and $\perp \hat{c}$ directions. In the present data on the organic superconductor, while the data do obey a \sqrt{H} behavior at fields $H \ll H^*(T)$, a clear departure is observed at fields H comparable to $H^*(T)$. Thus a more complete treatment seems to be called for.

Recently, Coffey and Clem [8] have worked out the high-frequency response of vortices including the effects of flux activation, based upon earlier results [16] exploiting the analogy of the equation of motion to that of a Brownian particle in a periodic potential $U = U_0[1 - \cos(2\pi x/L)]$. They show that the mobility can be expressed as

$$\begin{aligned} \bar{\mu}(\omega, T) &= \eta^{-1} (1 + \{i\omega\tau_0/\alpha + 1/[I_0^2(\nu) - 1]\}^{-1})^{-1} \\ &= \eta^{-1} g(\omega\tau_0, \nu), \end{aligned} \quad (2)$$

where $\nu = U_0/2k_B T$, the relaxation time $\tau_0 = \eta/\kappa\rho$, and $\alpha = I_1(\nu)/I_0(\nu)$. The mobility is related to the complex resistivity via $\bar{\rho}_r = \phi_0 B \bar{\mu}$.

From the J - E relation $J_\omega = \bar{\rho}_r^{-1}(\omega) E_\omega$, one obtains a complex penetration depth

$$\tilde{\lambda}_r^2(\omega, B, T) = \bar{\rho}_r(\omega, B, T)/(i\omega\mu_0) = \phi_0 B \bar{\mu}/(i\omega\mu_0). \quad (3)$$

Using a functional form for the barrier height $U_0(B, T) = A(T)/B$, then $\nu = A(T)/2k_B T B \equiv B^*(T)/B$, where $B^*(T) = A(T)/2k_B T$. From the above equations the penetration depth can be expressed as

$$\begin{aligned} \lambda_r(B, T, \omega) &= \text{Re}[\tilde{\lambda}_r(B, T, \omega)] \\ &= \delta^*(T) \text{Re}[ixg(\omega\tau_0, x^{-1})]^{1/2} \\ &\equiv \delta^*(T) h(\omega\tau_0, x), \end{aligned} \quad (4)$$

where $x = 1/\nu = B/B^*(T)$ and $\delta^*(T) = [\phi_0 B^*(T)/\mu_0 \omega \eta]^{1/2}$, which may be regarded as the flux-flow skin depth when $H = H^*(T)$.

It is apparent from Eq. (4) that the vortex contribution to the penetration depth can be represented in terms of a length scale $\delta^*(T)$ and a field scale $B^*(T)$ —both features which are contained in the data of Figs. 1 and 2.

It is useful to examine limiting cases predicted by the theory. In the limit of low fields $H \ll H^*(T)$, i.e., $x \rightarrow 0$, the penetration depth reduces to the pinning penetration depth given by Eq. (1). At high fields $H \gg H^*(T)$, i.e., $x \rightarrow \infty$, where the vortices essentially ignore the pinning potential due to thermal agitation, the penetration depth becomes the flux-flow skin depth, i.e., $\lambda_r = (\phi_0 H/\mu_0 \eta \omega)^{1/2}$. (This is essentially because the mobility increases from a low-field plateau to a high-field plateau, due to the increasing importance of thermal agitation.) Thus the field dependence of λ in both the high- and low-field limits is $\lambda \propto \sqrt{H}$. However, there is a crossover as the external field traverses the "depinning" field. It is important to note that this crossover can only be obtained by inclusion of the thermal agitation, and ignoring it leads only to a single \sqrt{H} behavior for the fixed-frequency experiment discussed here. The complete behavior for all fields can only be obtained by numerical computation.

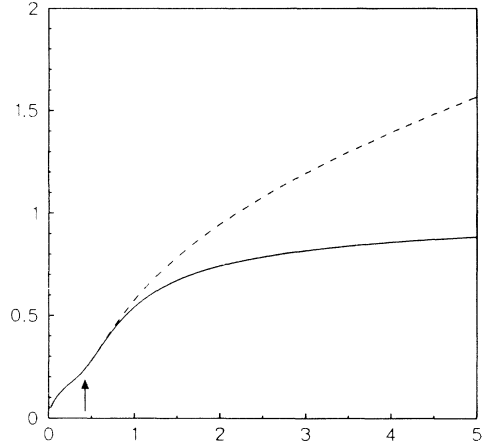


FIG. 4. Plots of the theoretical $\lambda_r(H, T)/\delta^*(T)$ vs $H/H^*(T)$ (dashed line) and $[\lambda_r(H, T)/\delta^*(T)] \tanh[\delta^*(T)/\lambda_r(H, T)]$ (solid line). The arrow indicates the crossover region. This is to be compared with the experimental data in Fig. 3.

The calculated dependence of $\lambda_r/\delta^*(T)$ vs $H/H^*(T)$ is shown in Fig. 4 as the dashed line. The value of $\omega\tau_0 = 0.1$ was used for the particular curve shown. The limiting \sqrt{H} behavior at low and high fields but with different slopes, which was discussed above, is evident from the detailed calculation. It is clear that the calculated curve has the same behavior as the scaled data shown in Fig. 2. In particular the low-field dependence and, most importantly, the crossover which appears as a kink at about $H/H^*(T) \sim 0.5$ are present in both experiment and theory, and are shown by the arrows in Figs. 2 and 4. Above this crossover, both the experiment and theory increase at a faster rate; however, the scaled experimental data ultimately saturate. This feature is not contained in the above model, according to which in this depinned regime the penetration depth should increase as \sqrt{H} (just as the flux-flow skin depth does). Thus it appears that for $H \gg H^*(T)$, the monotonic divergence (as \sqrt{H}) of the penetration depth is cut off (see Fig. 2) although the scaling behavior is retained.

In order to understand this cutoff, it is necessary to examine the $H=0$ data. These are presented in the form $\lambda(T_c) - \lambda(0, T)$ vs T in Fig. 5. Although the data appear to obey the conventional behavior commonly seen in superconductors, we have not found it possible to obtain good fits with the two-fluid model or the BCS model. Instead the data are remarkably connected to the finite H data, as is shown by also plotting $\Delta\lambda^*(T)$ in Fig. 5. The close correspondence between $\Delta\lambda^*(T)$ and $\lambda(T_c) - \lambda(0, T)$ suggests that the zero-field data are determined by the same length scale as the $H \neq 0$ data.

This also provides an explanation for the saturation in the data at large fields. The effective change in penetration depth cannot increase without limit, and one might expect that it cannot exceed $\lambda(T_c) - \lambda(0, T)$ [and hence $\Delta\lambda^*(T)$]. We have found that a functional form $[\lambda_r/\delta^*(T)] \tanh[\delta^*(T)/\lambda_r]$ is a reasonably good descrip-

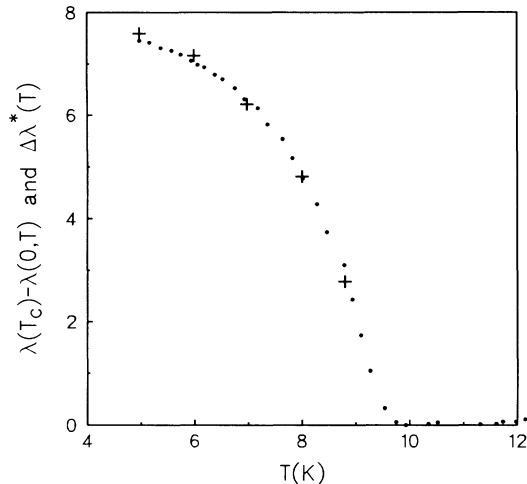


FIG. 5. $\lambda(T_c) - \lambda(0, T)$ vs T (represented by solid circles) and $\Delta\lambda^*(T)$ vs T (represented by crosses).

tion of the data, as shown by the solid line in Fig. 4. (The calculated curves are presented on a separate figure from the experiment for the sake of clarity.) It is important to note that the scaling behavior is retained even with the above cutoff, due to the close correspondence between the $H=0$ and $H \neq 0$ data.

We now turn to examining the implications of the analysis. The fact that a single parameter $\omega\tau_0=0.1$ is adequate (it is necessary for the scaling approach to work) implies a temperature-independent relaxation frequency $f_0=1/2\pi\tau_0=60$ MHz. The magnitude is comparable (~ 100 MHz) to that observed in other low- T_c superconductors. Since $\tau_0=\eta/\kappa_p$, the temperature independence of τ_0 implies that both η and κ_p have the same temperature dependence.

The above analysis also yields an estimate of the vortex activation energies. The observed temperature dependence of $H^*(T)$ yields for the pinning potential $U_0(t)=A(1-t)^{3/2}/B$. This form has been suggested [14] for the high- T_c superconductors based upon dc resistivity measurements. From $U_0=2k_B T[H^*(T)/H]$, we get $A=4$ KT. For comparison, dc resistivity measurements [17] yield $A \sim 2 \times 10^4$ KT for single-crystal YBCO, and 300 KT for Bi-Sr-Ca-Cu-O. Again the value of A is comparable to polycrystalline YBCO rather than single crystals. The low values of the potential are consistent with the importance of thermal fluctuations in this material.

Finally, we return to the zero-field state. Including the observed temperature dependence of $\lambda(0, T)$, both the $H=0$ and $H \neq 0$ data can be represented by $\lambda(T_c) - \lambda(H, T) = \Delta\lambda^*(T)[1 - f(H/H^*(T))]$; i.e., as noted above, the zero-field data are also governed by the same length scale as the data for finite H . In view of the previous discussion in which we associate $\Delta\lambda^*(T)$ with $\delta^*(T)$, this suggests that the zero-field state is not a conventional Meissner state, but rather is governed by the same features as the mixed state. This becomes clearer

from the expression $\lambda(0, T) = \lambda(T_c) - \Delta\lambda^*(T) = \lambda(T_c) - \delta^*(T)$. This suggests that the so-called penetration depth $\lambda(0, T)$ is really analogous to a flux-flow skin depth. This may be contrasted to a conventional superconductor, in which the electrodynamics in the Meissner and mixed states are governed by entirely different length scales. The likely possibility is that vortexlike excitations are present even in the zero-field state [18]. This possibility has been recognized by Hebard *et al.* [19], who have proposed vortex nucleation at defects to account for the anomalous temperature dependence in this material in terms of a pinning penetration depth, although our interpretation differs from those authors in that we suggest a flux-flow skin depth. This also suggests that earlier interpretation of electromagnetic data in terms of s - or p -wave states should be reexamined, since the above arguments indicate that the zero-field state below T_c may not obey a London relation with an accompanying Meissner effect.

To our knowledge, this is the first observation of scaling in the high-frequency response of the mixed state of a superconductor, which displays features commonly associated with the dc resistivity. The observed phenomenology appears to be characteristic of an extreme type-II superconductor, and should be observable in other layered superconductors.

We thank J. R. Clem for useful discussions. Work at Northeastern was supported by a grant from Rome Laboratories, Hanscomb AFB, and U.S. AF.

- [1] A. M. Kini *et al.*, *Inorg. Chem.* **1990**, 2555.
- [2] K. Kanoda *et al.*, *Phys. Rev. Lett.* **65**, 1271 (1990).
- [3] D. R. Harshmann *et al.*, *Phys. Rev. Lett.* **64**, 1293 (1990).
- [4] O. Klein *et al.*, *Phys. Rev. Lett.* **66**, 655 (1991).
- [5] D. E. Farrell *et al.*, *Phys. Rev. B* **42**, 8694 (1990).
- [6] G. Saito, *Physica (Amsterdam)* **162-164C**, 577-582 (1989).
- [7] P. W. Anderson and J. R. Schrieffer, *Phys. Today* **44**, 55-61 (1991).
- [8] M. W. Coffey and J. R. Clem, *Phys. Rev. Lett.* **67**, 386 (1991).
- [9] H. Urayama *et al.*, *Chem. Lett.* **1988**, 55.
- [10] Dong-Ho Wu and S. Sridhar, *Phys. Rev. Lett.* **65**, 2074 (1990).
- [11] S. Sridhar, Dong-Ho Wu, and W. Kennedy, *Phys. Rev. Lett.* **63**, 1873 (1989).
- [12] K. A. Müller, M. Takashige, and J. G. Bednorz, *Phys. Rev. Lett.* **58**, 1143 (1987).
- [13] A. F. Hebard *et al.*, *Phys. Rev. B* **40**, 5243 (1989).
- [14] M. Tinkham, *Phys. Rev. Lett.* **61**, 1658 (1988).
- [15] Y. Yeshurun and A. P. Malozemoff, *Phys. Rev. Lett.* **60**, 2202 (1988).
- [16] W. R. Schneider, *Z. Phys. B* **24**, 135 (1976).
- [17] T. T. M. Palstra *et al.*, *Appl. Phys. Lett.* **54**, 769 (1989).
- [18] D. Fisher, M. P. A. Fisher, and D. Huse, *Phys. Rev. B* **43**, 130 (1991).
- [19] A. F. Hebard *et al.*, *Phys. Rev. B* **44**, 9753 (1991).